The Impact of Nano-fluid Concentration Used as an Engine Coolant on the Warm-up Timing

M. Eftekhar[1], A. Keshavarz[2] A. Ghasemian[3], and J. Mahdavinia[4]

[1] MSc Graduate [2] Associate Professor [3] Ph.D Student [4] MSc Gratuate Faculty of Mechanical Engineering, K.N. Toosi University of Technology

*keshavarz@kntu.ac.ir

Abstract

Running the industrial components at a proper temperature is always a big challenge for engineers. Internal combustion engines are among these components in which temperature plays a big role in their performance and emissions. With the development of new technology in the fields of 'nano-materials' and 'nano-fluids', it seems very promising to use this technology as a coolant in the internal combustion engines. In this study, a nano-fluid (Al2O3-Water/Ethylene Glycol (EG)) is used as an engine coolant along with an optimized heat exchanger to reduce the warm-up timing. The effect of nano-fluid concentration is considered here by using their corresponding governing equations, such as momentum and energy. The engine coolant thermal behavior calculation is carried out based on the lumped method. The obtained results indicated that using different percentage of nano-fluid mixtures (by volume), such as Al2O3-Water/EG as engine coolant enhances the heat transfer coefficient and reduces the warm-up timing which, in turn, results in reduced emissions and fuel consumption.

Keywords: Nano fluid, internal combustion engine, warm-up timing, emission and fuel consumption reduction.

1. INTRODUCTION

Due to the environmental regulations, such as Euro 5 and 6 legislations, Ultra Low Emission Vehicle (ULEV) and Federal Test Procedure (FTD) emission standards, nowadays a great deal of attention has been directed towards to environmental hazards and energy conservation. Researchers have shown that sixty percent of the world air pollutions are due to the transportation among which more than fifty per cent of them are related to the warm-up period of an internal combustion engine [1].

During the cold start of a spark ignition (SI) engine, the friction loss is more than two times of the steady state conditions. Because of the incomplete combustion and the high friction, the additional fuel is injected to burn the rich mixture of air/fuel during a cold start [2], so the fuel consumption and the exhaust emissions, such as carbon monoxide (CO) and total hydrocarbon (THC) would increase [3]. In fact, reducing the warm-up period can extremely decrease the fuel consumption and the exhaust emissions [4]. Although the integration of an exhaust manifold with a cylinder head, along with some valve timing modifications, has proved to be a very promising method to fulfill the above issues, but it requires major modifications, especially in the manufacturing production lines [5-7].

Four optimum heat exchangers as shown schematically in Figure 1 are separately designed and installed before and after the close-coupled catalytic converter on a spark ignition engine to reduce the warm-up timing by Eftekhar & Keshavarz [8]. Since the overall schematic of the four heat exchangers is similar, only one general Figure of the heat exchanger is shown in two different orientations. The specifications of each heat exchanger are given in Table 1. A summary of the engine specifications which was considered in their article is given in Table 2. The heat exchanger installed before the catalyst cools the exhaust gas temperature at high loads. It had a similar impact on the exhaust gas temperature as an exhaust gas recirculation (EGR) cooler [4, 9,10]. On the contrary, positioning the heat exchangers after the catalyst helps to heat up the coolant without consuming any extra energy which, in turn, results in a lower warm-up period. Although placing the heat exchangers in the exhaust gas stream does increase the back pressure, the study proved that the increase

was not significant enough to affect the engine performance nor did it have any significant effect on the light-off time [11]. The first and second laws of thermodynamics (energy and exergy) were applied to optimize the heat exchanger dimension, with respect to the back pressure and the heat transfer effect, which led to a minimum pressure drop with a maximum heat transfer.

A nano-fluid is achieved by dispersing nano-particles in a base-fluid. One of the main goals of producing nano-fluids is to enhance the fluid heat transfer. Suspended nano-particles have higher thermal conductivity than base-fluids, so the effective thermal conductivity of the nano-fluids increases. Choi et al [12] showed that the addition of a small amount of nano-particles (less than 1% by volume) to base fluid would increase the thermal conductivity of the fluid up to approximately two times. The thermal conductivity of nano-fluids strongly depends on the volume fraction and properties of nano-particles. It is not easy to accurately determine the thermal conductivity of nano-fluids by a single formula, but there are some experimental relations that could be used to estimate it. Due to the enhancement of the thermal conductivity of the nano-fluids, the convective heat transfer coefficient of the nano-fluids increases, too. The enhancement of convective heat transfer coefficient of a nano-fluid in an internal flow has been reviewed by Wang [13] in both laminar and turbulent regimes.

A mixture of ethylene glycol and water is used mostly as the coolant in internal combustion engines. Therefore, Water/EG is used as base-fluid in this study. Engine coolant is made by 50% EG and 50% water volume fraction; and all of the fluid properties are calculated based on this 50/50 concentration. Al2O3 is used as nano-particles that are dispersed in

base-fluid. The new coolant (nano-fluid) improves the heat exchanger/radiator performance. These benefits improve the performance of heat exchangers and heat devices which, in turn, leads to the reduction of weight and size of the water pump and eventually increases the cooling effectiveness and the engine power.

The heat transfer characteristics of Water/EG-Al2O3 is evaluated in a turbulent regime. Scientific studies in the field of nano-fluid have already showed that there are two methods for analyzing the hydraulic and heat transfer behaviors of nano-fluids [14,15].These two methods include a single phase and two phases. In the single phase, it is supposed that the nano-particles have same velocity with the base-fluid molecules and are in thermal equilibrium. So in this model, the nano-fluid is considered similar to the base-fluid with new thermo physical properties. In the other model, the nano-particles are considered as a separate phase that can be in different velocity and temperature as compared to the base-fluid. In the latter method, the motion of nano-particles is determined by the Newton's second law of motion that is more complicated than the previous one and is called Lagrangian trajectory method. Many recent researches have showed that a nano-fluid with a low concentration can be analyzed with a single phase method [16, 17].

In this study, a nano-fluid (Al2O3-Water/EG) is utilized as the engine coolant. The specifics of the engine is given in Table 2. The nano-fluids thermo physical properties are calculated by a single phase method similar to that of Ghasemian[18]. The engine coolant thermal behavior in the warm-up period is simulated by lump method. The effect of nano-fluid concentration on the warm-up timing is considered when the heat exchangers are utilized along with the exhaust gas streamline.
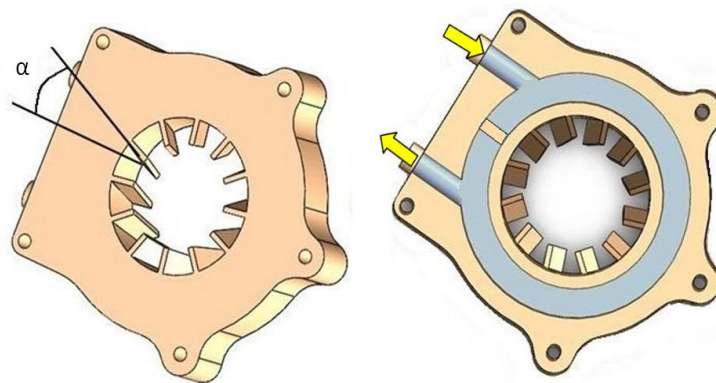

Fig1.schematic of finned-tube heat exchangers in two different orientations

Table 1. Heat exchangers specifications [28]

Parameters	Medium fin	High fin	Micro fin	Spirally fluted tube
Maximum diameter, D_i (mm)	68	68	68	68
Fin height, e (mm)	12.2	4.1	1.37	10.7
Fin thickness ,t (mm)	1.21	1.46	0.22	1.16
Number of fns, n_f	8	16	40	24
Helix angle of fin (α)	30°	30°	30°	30°
Heat exchanger length, L (mm)	200	200	200	200

Table 2. The engine specifications

Cylinder	4
Bore (mm)	78.6
Stroke (mm)	85
Displacement (cc)	1650
Compression ratio	11.2

2. Calculations

a. Thermal behavior simulation of the coolant

The warm-up timing is a transient thermal period in which the temperature of the engine and its components would increase from the environmental temperature to the engine operational temperature. Therefore, it cannot be analyzed as a steady state heat transfer and it should be considered by a transient heat transfer such as the lumped method. Many researchers have shown that this method is very accurate [2, 19 & 20]. Ghasemian and Jazaiery [19] considered the engine coolant thermal behavior when the coolant, oil and engine components were preheated, using electrical energy. They showed that preheating the coolant is the most effective technique to reduce the warm-up period. The engine coolant thermal behavior calculation in this study is carried out based on the lumped method similar to [19]. To simulate the thermal behavior of the engine, it is divided into 7 main parts; Piston, cylinder block, cylinder head, oil, cylinder block coolant, cylinder head coolant and the coolant that exists between the cylinder head exit and cylinder block inlet as shown in Figure 2. The heat transfer equation of each part is derived by applying conservation of energy. The eight time dependent differential equations (equation (1)-

(8)) are achieved in terms of the relevant energy and solved numerically:

$$\frac{dT_{pi}}{dt} = \left[\frac{1}{(mC)_{pi} + (mC)_{con}}\right] \times (\dot{Q}_{pi} - \dot{Q}_{pi-oil} - \dot{Q}_r - \dot{Q}_{con})$$
(1)

$$\frac{dT_{bl}}{dt} = \left[\frac{1}{(mC)_{bl}}\right]\left[\dot{Q}_{bl} + \dot{Q}_r - \dot{Q}_{bl-cool} - (hA)_{bl}(T_{bl} - T_{amb})/dt\right]$$
(2)

$$\frac{dT_{hd}}{dt} = \left[\frac{1}{(mC)_{hd}}\right] \times \left[\dot{Q}_{hd} + \dot{Q}_{exh} + \dot{Q}_{vtr} - \dot{Q}_{hd-cool} - (\dot{m}C)_{oil}(T_{oil} - T_{oil-in})\right]$$
(3)

$$\frac{dT_{oil}}{dt} = \left[\frac{1}{(mC)_{oil+cr}}\right] \times \left[\begin{array}{l} \dot{Q}_{pi-oil} + \dot{Q}_{hd-oil} + \dot{Q}_{vtr} + \dot{Q}_{fr-op} + \dot{Q}_{fr-cr} \\ + \dot{Q}_{con} - (hA)_{oil-amb}(T_{oil} - T_{amb})/dt \end{array}\right]$$
(4)

$$\frac{dT_{bl-cool}}{dt} = \left[\frac{1}{(mC)_{bl\ coolant}}\right] \times (\dot{Q}_{bl-cool} - \dot{Q}_{bl-cool\ flow})$$
(5)

$$\frac{dT_{hd-cool}}{dt} = \left[\frac{1}{(mC)_{hd\ coolant}}\right] \times (\dot{Q}_{hd-cool} - \dot{Q}_{hd-cool\ flow})$$
(6)

$$\frac{dT_{bl\ cool\ in}}{dt} = \frac{dT_{hd\ cool\ out}}{dt}$$
(7)

$$\frac{dT_{bl-coolin}}{dt} = \left[\frac{1}{m_{radcool}C_{bl\ cool} + m_{rad}C_{rad} + m_{cool}\frac{(C_{bl\ cool} + C_{hd\ cool})}{2}}\right] \times$$
$$\left[\dot{Q}_{wp} + E_{rad}C_{min}(T_{amb} - T_{hd\ cool}) - \dot{m}_{cool}C_{bl\ cool}(T_{bl-in} - T_{hd})\right]$$
(8)

It should be noted that equation (7) is utilized when the coolant temperature is less than that of the thermostat operative temperature (when the thermostat is closed) whereas equation (8) is used for

other conditions. It means that based on the coolant temperature of the cylinder head outlet either equations (1-7) or (1-6 & 8) are solved simultaneously. The obtained results are validated with some available experimental data of [19]. Figure 3 shows the experimental and simulated values of the coolant temperature in terms of time. As the experimental data (green line) shows, the coolant temperature has reached 353 K where the thermostat opens for the first time and then the engine reaches its steady state condition after 182 seconds, while the simulated values indicate that the same temperature is

reached after 172.8 seconds, which shows an error of about 5%. The peak points of the graphs show the time when the thermostat opens.

b   Heat exchanger optimization

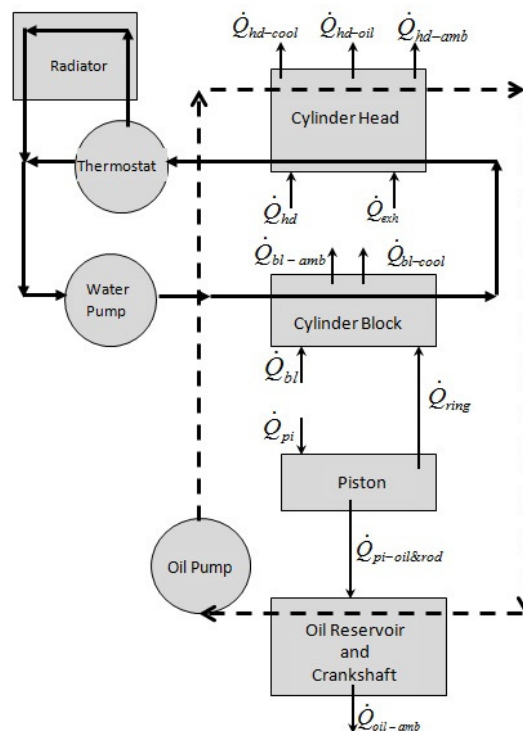Four different types of heat exchangers with internally helical fins as shown in Figure 1 are considered here.
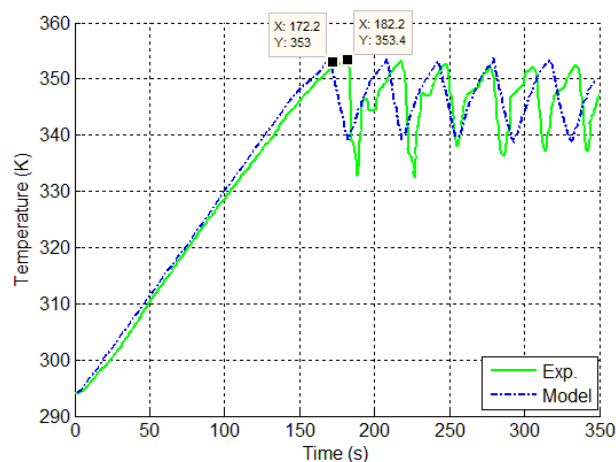.

Fig2. The physical model of engine

Fig3. The experimental and the simulated data variation of the coolant temperature in terms of time [19]

Three of them are internally finned tubes while the fourth one is a spirally fluted tube the same as [8]. The heat exchangers are analyzed and optimized based on both the first and second laws of thermodynamics. The rate of the calculated entropy generation of the flow is used to optimize the heat exchangers similar to that of Bejan`s work [21], e.g. the entropy generation rate minimization. In this study, the analysis is performed for the flow passage through an arbitrary cross-section as shown in Figure 4. A differential element dx of the flow is taken as the system. Then, the rate of entropy generation for this system can be written as:

$$d\dot{S}_{gen} = \dot{m}ds + \frac{q'dx}{T - \Delta T}$$
(9)

By using the energy equation and the canonical relation, simplifying and defining dimensionless parameters, such as ReD, the entropy generation rate can be expressed as equation (10):

$$\dot{S}'_{gen} = \frac{q'^2}{\pi k_f T^2 Nu(Re_{d_h}, Pr)} + \frac{32\dot{m}^3}{\pi^2 \rho^2 T} \cdot \frac{f(Re_{d_h})}{d_h^5}$$
(10)

Where

$$\dot{S}'_{gen} = \frac{d\dot{S}_{gen}}{dx}$$
(11)

Substituting equation (11) into equation 10:

$$\dot{S}'_{gen} = \frac{q'^2}{\pi k_f T^2 Nu(Re_{d_h}, Pr)} + \frac{\mu U^3}{2\pi T} \cdot \frac{Re_{d_{im}}^6}{Re_{d_h}^5} \cdot f(Re_{d_h})$$
(12)

The first term at the right hand side of equation (12) indicates the heat transfer where the second term correlates with the pressure drop of the flow in the duct. The friction factor and heat transfer coefficient can be obtained by solving the related governing equations, namely continuity, momentum and energy equation with different boundary conditions. But the varieties of dimension parameters provide a new set of boundary conditions which cannot be achieved by the pervasive analytical correlations. Fortunately, many researchers have developed empirical correlations for the Nusselt number and the friction factor for the turbulent flow in the internally finned tubes and spirally fluted tubes. Figure 5 shows the dimensional parameters for the finned tubes. Based on the fin height, the number of fins and the fin thickness [22], these tubes are classified into the following groups, micro, medium and high finned tubes. The Nusselt number and friction factor correlations for each type of the tubes were experimentally obtained and presented in [22-27].
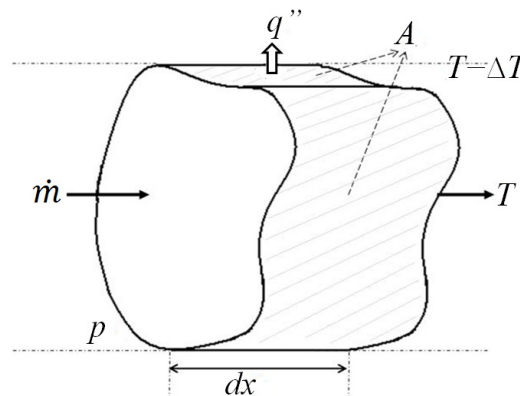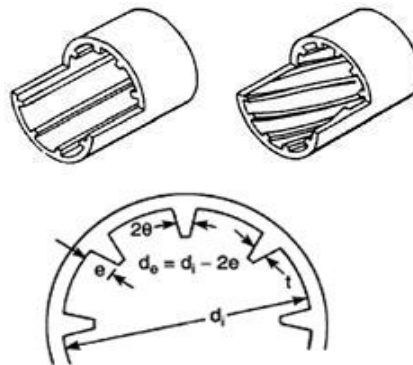
Fig4. An arbitrary cross-section of the flow

Fig5. Dimensional parameters for the fins [22]

Finally, the equations of entropy generation rate are obtained by substituting the corresponding correlations of the Nusselt number and friction factor into equation (12). For example, the entropy generation rate of the medium fins is calculated by equation (13) which is obtained from the substitution of the Nusselt number and friction factor relations into equation (12) along with some simplifications [8]:

$$\dot{S}'_{gen} = \frac{q'^2}{0.023 \pi k_f T^2} \cdot \frac{\cos \alpha^3}{Re_{d_i}^{0.8} Pr^{0.4}} \left(1 + \frac{2}{\pi} n_f \frac{Re_e}{Re_{d_i}}\right)^{0.5} \left[\frac{Re_{d_i} - 2 Re_e}{\sqrt{Re_{d_i}^2 - \frac{4}{\pi} Re_e Re_t}}\right]^{0.2}$$
$$+ \left(\frac{\mu U_\infty^2}{2\pi^4 T}\right) \frac{(\pi Re_{d_i} + 2 n_f Re_e)^3}{\left(Re_{d_i}^2 - \frac{4}{\pi} n_f Re_e Re_t\right)^{2.5}} \cdot [0.046 \sec \alpha^{0.75} Re_{d_i}^{0.8}] \quad (13)$$

Three similar equations are obtained [28] for the other fins. By assuming the values of maximum diameter (di), fluid velocity (U∞), fluid density (ρ), thermal conductivity of fluid (k), Prandtl number (Pr), viscosity of fluid (μ) and helix angle of fin (α) as constant values, only three variable parameters, namely number of fins (n_f), fin height (e) and thickness (t) remain in all the entropy generation rate equations, such as equation (13). Taking the derivative of the entropy generation rate, $\dot{S}'_{gen}$, of each state with respect to each of the variable parameters and setting them to zero, leads to four sets of equations which are as follows:

$$\begin{cases} \dfrac{\partial \dot{S}'_{gen}}{\partial Re_e} = 0 \\ \dfrac{\partial \dot{S}'_{gen}}{\partial Re_t} = 0 \\ \dfrac{\partial \dot{S}'_{gen}}{\partial n_f} = 0 \end{cases} \quad (14)$$

The equations are nonlinear. These sets of nonlinear equations are solved numerically by using in house developed package along with the Matlab® software. It should be noted that the value of q' is updated using equation (15) in each step.

$$q' = h_{d_h}\big|_{ave} A_p (T_{ave,gas} - T_{wall}) \quad (15)$$

Where the heat transfer coefficient is obtained from:

$$Nu_{d_h}\big|_{ave} = \frac{d_h h_{d_h}\big|_{ave}}{k} \quad (16)$$

The calculations are performed, using the exhaust gas properties at the cold start conditions after the catalyst outlet as given in Table 3.

After solving the set of equations for each heat exchanger, the optimum heat exchangers will be resulted as Table 1[28]:

It is noteworthy that throughout these calculations, the exhaust gas properties are assumed to be constant. The mass flow rate which passes through the heat exchanger is calculated, using equations (17) and (18) as presented in [3]:

$$\dot{m}_{a,in} = \eta_v \rho_{in} V_d \frac{N}{60 \times 2} \text{(number of cylinders)} \quad (17)$$

$$\dot{m}_{in} = \dot{m}_{a,in}\left(1 + \frac{1}{AF}\right) \quad (18)$$

The exhaust gas velocity is calculated for the continuity equation as:

$$\dot{m}_{in,engine} = \dot{m}_{out,engine} \quad (19)$$

$$\dot{m}_{out,engine} = \rho_{ex}.A_{cross}.U_{ex} \quad (20)$$

c   Nano fluid

There is no theoretical formula currently available to precisely determine most of the thermo physical properties of nano-fluid. The equations used in this simulation are as follows: the subscripts bf, nf and p refer to the base fluids, the nano-fluids and the particles, respectively.

Thermal conductivity:

Several semi-empirical correlations are stated by researchers to express the thermal conductivity. The most commonly used equation among them is proposed by Hamilton and Crosser [29]:

$$\frac{k_{nf}}{k_{bf}} = \frac{k_P + (n-1)k_{bf} - (n-1)\varphi(k_{bf} - k_P)}{k_P + (n-1)k_{bf} + \varphi(k_{bf} - k_P)} \quad (21)$$

Table 3 The properties of the exhaust gas at cold start

T_{gas}:	130° C	k_f:	0.055 W/mK
U:	4.89 m.s^{-1}	p:	101 kPa
c_p:	1014 J/kg.K	μ:	10^{-5} N.s/m^2
ρ:	0.8711 kg.m^{-3}	Pr:	0.69

In the above equation, n is the empirical shape factor which accounts for the effect of the shape of the particles and is equal to 3 for spherical nano-particles.

Dynamic Viscosity:

In this work, the dynamic viscosity of Al2O3 (50nm)/EG-Water nano-fluid with volume concentration of 1, 2 and 3% is considered to be dependent on the volume concentration and is calculated by the relation developed by [30]:

$$\mu_{nf} = 0.904 \exp(0.1483\varphi).\mu_{bf} \qquad (22)$$

Density:

The density of nano-fluids is calculated by [31]:

$$\rho_{nf} = \varphi\rho_P + (1-\varphi)\rho_{bf} \qquad (23)$$

Specific Heat:

The following equation is used for the specific heat capacity [32]:

$$\rho_{nf}C_{nf} = \varphi\rho_P C_P + (1-\varphi)\rho_{bf}C_{bf} \qquad (24)$$

Although the properties of base fluid (Water/EG) and nano-particles depend on the temperature but due to the small variation of temperature across the engine (about 10K), their properties are calculated at temperature 350K [33,34].

In Table 4, the thermo physical properties of the base fluid, the nano-particle and the nano-fluids for volume concentrations of 1%, 2% and 3% are presented.

3. Results and Discussion

a. Pressure Drop

By increasing the density and viscosity of fluid flow, its pressure drop increases which results in higher consumption of pump power. By knowing the Reynolds (Re) number and relative roughness of the tube (es/dh), the friction factor of different turbulent flows inside the tube can be calculated by using the Moody diagram or equation (25) [35].

$$f_{d_h} = \frac{0.25}{\left\{\log\left[\left(\frac{e_s}{3.7d_h}\right)+\left(\frac{5.74}{\text{Re}_{d_h}^{0.9}}\right)\right]\right\}^2} \qquad (25)$$

Equation (25) is valid for $5\times10^3 \le \text{Re}_{dh} \le 10^8$ and $10^{-6} \le es/dh \le 10^{-2}$, which is suitable for this study. In equation (25), the Fraction of es/d_h is constant, es which is the tube roughness value is taken as 0.26 mm (cast iron), and the Reynolds number, Re_{dh} is the only variable. The head loss hl is defined based on the Darcy-Weisbach and pressure drop can be found from equations (26) & (27), respectively.

$$h_l = f_{d_h}.\frac{L}{d_h}.\frac{U_\infty^2}{2} \qquad (26)$$

$$\Delta P = \rho.\left(\frac{0.25}{\left\{\log\left[\left(\frac{e_s}{3.7d_h}\right)+\left(\frac{5.74}{\text{Re}_{d_h}^{0.9}}\right)\right]\right\}^2}\right).\frac{L}{d_h}.\frac{U_\infty^2}{2} \qquad (27)$$

Table 3 The properties of the exhaust gas at cold start

T_{gas}:	130° C	k_f:	0.055 W/mK
U:	4.89 m.s^{-1}	p:	101 kPa
c_p:	1014 J/kg.K	μ:	10^{-5} N.s/m^2
ρ:	0.8711 kg.m^{-3}	Pr:	0.69

Table 4: Base fluid, nano particle and nano fluids thermo physical properties

Type of material	Volume concentration (%)	Density (kg/m3)	Specific Heat (J/kg K)	Thermal conductivity (W/m K)	Viscosity (m Pa s)
Al$_2$O$_3$	-------	3950.00	873.336	31.922	----
Water/EG (base fluid)	0	1024.780	3645.397	0.41296	0.8920
Al$_2$O$_3$-Water/EG	1	1054.976	3552.637	0.42354	0.9353
Al$_2$O$_3$-Water/EG	2	1084.219	3454.039	0.43577	1.0848
Al$_2$O$_3$-Water/EG	3	1113.462	3360.621	0.44824	1.2582

Table 5 gives the values of pressure drop (ΔP) in a tube for different nano-fluid concentrations. By increasing the nano-fluid concentration, its kinematic viscosity increases which leads to a lower Reynolds number. Thus, the value of friction coefficient, fd increases which produces higher head loss with the assumption of constant mean velocity.

Table 5. The pressure drop in path for different percentage nano fluid

Volume concentration	ΔP (Pa)
0	147.907
1	152.428
2	157.82
3	163.628

According to equation (27), the value of pressure drop can be lower by reducing the value of mean velocity. Hence, to keep the input pumping power unchanged, the mean velocity may be changed as given in Table 6. Despite the mean velocity reduction, the mass flow rate increases slightly due to the density growth rate.

Table6. The mean velocity and mass flow rate of different percentage of mixture.

Volume concentration	Density (kg/m3)	$\dfrac{U_{\infty new}}{U_{\infty basefluid}}$	$\dfrac{\dot{m}_{\infty new}}{\dot{m}_{\infty basefluid}}$
0	1024.780	1	1
1	1054.976	0.9850	1.014
2	1084.219	0.9681	1.024
3	1113.462	0.9508	1.033

b. Warm-up Simulation

The heat exchanger operates for a short time during the engine cold start and then shuts off. Three different cold start heat exchanger operation times are applied to each of the heat exchangers to investigate their impact on the warm-up period similar to [8]. The simulations are preformed with the assumption that the heat exchanger operates until the coolant temperature is elevated by 5 K, 10 K whereas for the third case, the operation continues until the coolant temperature reaches the thermostat temperature set point. In all of the above cases, the initial coolant and the engine components' temperature are assumed to be 293 K and the coolant mass flow rate is taken to be 16 liter/min at 1000 RPM. The value of new mass flow rate which includes the nano-particles is changed as given in Table 6.

The calculated results for the medium internally finned tubes are discussed here in detail as an example whereas for the other tubes, only the final calculated values are given. For the first case, after 49.3 seconds, the entire coolant (water/EG) is heated by 5 K and the warm-up period is reduced by 17.1 seconds in comparison to the engine with no heat exchanger as shown in Figure 6. The dash-dot line shows the shutting off time of the heat exchanger. When the nano-fluid with one, two and three percent mixture of the nano-particles is utilized as the coolant, the warm-up period is decreased to 18.3, 20.1 and 22.2 seconds, respectively. It means that the warm-up timing reduction has increased by 29.8% when 3% mixture nano-fluid is used as the engine coolant. Table 7 gives the warm-up timing reduction by utilizing the other heat exchangers.
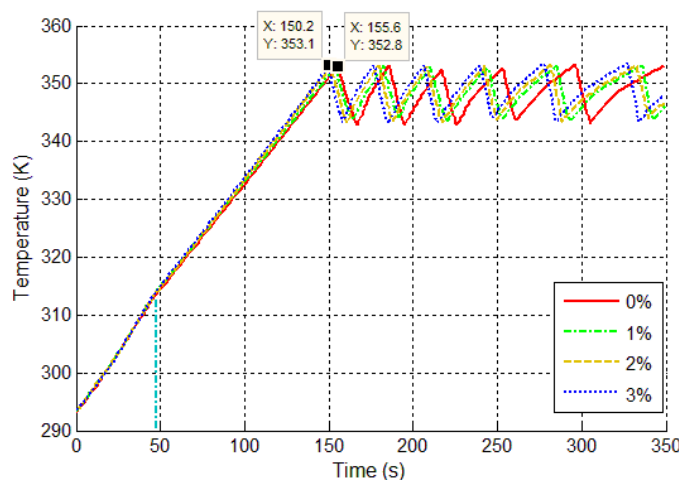

Fig6. Variation of coolant temperature in terms of time when coolant is heated by 5°C - Medium fins

Table 7 Warm-up period reduction for first simulated cases

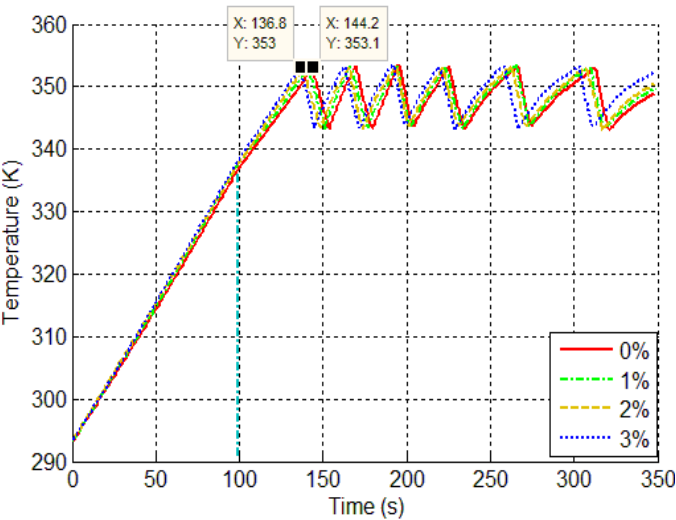| Heat exchanger type	Volume Concentration			
	0%	1%	2%	3%
Medium finned tubes	17.1	18.3	20.1	22.2
High finned tubes	16.7	17.9	19.63	21.5
Micro finned tubes	16.9	18.1	19.8	21.9
Spirally fluted tubes	18.1	19.31	21.3	23.5

Fig7. Variation of coolant temperature in terms of time when coolant is heated by 10°C - Medium fins

Table 8. Warm-up period reduction for second simulated cases

Heat exchanger type	Volume Concentration			
	0%	1%	2%	3%
Medium finned tubes	28.5	31.3	33	35.1
High finned tubes	27.2	30	31.6	33.7
Micro finned tubes	27.8	30.6	32.4	34.3
Spirally fluted tubes	31.1	34.2	36	38.4

For the second case, the coolant is heated by 10 K after 98.6 seconds. As a result, the warm-up time is decreased by 28.5 seconds in comparison to the engine with no heat exchanger as shown in Figure 7. Also, as the nano-particle concentration is increased, the warm-up period is reduced by 31.3, 33 and 35.1 seconds, respectively. Therefore, the warm-up reduction time increases to 23.1 percent by using 3% mixture nano-fluid. Table 8 shows the warm-up timing reduction by using the other heat exchangers for the same condition.

In the third case, when the heat exchanger stayed in the line until the thermostat started to function, the warm-up time is reduced by 38.5 seconds which is shown in Figure 8. The warm-up timing is decreased by 40.3, 41.1 and 42.8 seconds, respectively by the addition of nano-particles concentrations. Therefore, the reduction time is increased to 11.2 percent for the maximum nano-fluid concentration. Similarly, the simulation is performed for the other heat exchangers and the warm-up period reduction values are tabulated in Table 9.

As given in Tables 7 to 9, the spirally fluted tube leads to a decrease in the warm-up period more than the others in all the three cases. The pressure drop value of each heat exchanger was calculated [8]. The

spirally fluted tube produces the most pressure drop which may influence the engine performance. The medium finned tube provides the least pressure drop while it decreases the warm-up period more than that of the micro and high finned tube. Obviously, the other observation is that more heating of the coolant results in more reduction of the warm-up period.

The installed heat exchanger after the catalytic converter acts as a heater and it reduces the warm-up period without using any external energy. An engine usually runs with rich air-fuel mixture during the warm up timing to avoid misfire as well as to have more completed combustion. Also, it is well known that the total unburned hydrocarbons are very high during the cold start. Therefore, the warm up timing reduction leads to lower emission and fuel consumption as shown by [3] & [36]. It is worth mentioning that the exhaust gas temperature in the calculations was assumed to be 403 K where in reality the component temperature increases as the time passes by and results in higher exhaust gas temperature. That means the heat flux increases as time passes (which is not considered in the simulation) and reduces the warm-up period even more in the real time.

As the nano-fluid concentration increases, its specific heat decreases as given in Table 4. Therefore, according to equation (28), for a constant heat and mass flux, the coolant temperature increases as the nano-fluid concentration grows.

$$\dot{q} = \dot{m}c_p(T_e - T_i) \tag{28}$$

As expected, the enhancement of heat transfer coefficient leads to higher heat transfer which, in turn, lowers warm up timing as shown in Figures 5 to 7.
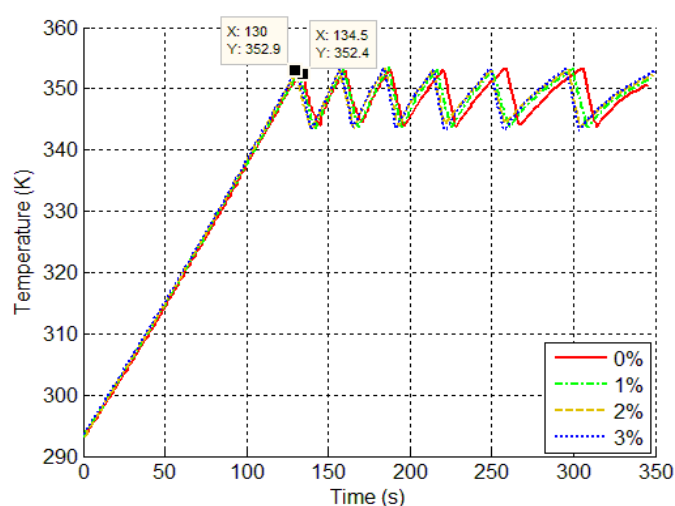

Fig8. Variation of coolant temperature in terms of time until the thermostat begins to act - Medium fins

Table. 9 Warm-up period reduction for third simulated cases

Heat exchanger type	Volume Concentration			
	0%	1%	2%	3%
Medium finned tubes	38.5	40.3	41.1	42.8
High finned tubes	35.77	37.44	38.3	39.4
Micro finned tubes	36.8	38.7	39.6	41
Spirally fluted tubes	47.5	49.9	51	53.1

4. Conclusion

The impact of nano-fluid concentration, used as internal combustion engine coolant, on the warm up timing was investigated numerically. Four different

finned types of heat exchangers are installed along the exhaust gas streamline for three different cases. Based on this study, the following conclusions can be drawn:

1. The maximum warm-up timing reduction is about 10.2% when 1% nano-particle is added into the based coolant. This reduction occurred on the high finned tubes.

2. The maximum warm-up timing reduction is about 17.2% when 2% nano-particle is added into the based coolant. This reduction occurred on the micro finned tubes.

3. The maximum warm-up timing reduction is about 29.8% when 3% nano-particle is added into the based coolant. This reduction occurred on the spirally fluted tubes.

Although the maximum percentage reduction rate for 1% and 2% nano-fluid did not take place in the spirally fluted tubes, still the maximum warm-up timing reduction occurred in this type of heat exchanger for all the three cases. These reductions indirectly reduce the exhaust emissions and fuel consumption.

References:

[1]. Shahbakhti. M,. " Dynamic Modeling of MPFI for Air Fuel Ratio Control During Cold Start and Warm-up Conditions & Investigation Of Effective Factors on Air-Fuel Ratio Mixture Preparation, Pollutants Formation Mechanisms and Emission Reduction Methods in Cold Start and Warm-up Conditions", M.Sc Thesis of mechanical engineering of K.N.T. University of Technology, 2002.

[2]. Shayler, P. J. and Christian, S. J., "A Model for the Investigation of Temperature, Heat Flow and Friction Characteristics During Engine Warm-Up" SAE 931153, 1993.

[3]. Heywood, J.B, "Internal Combustion Engine Fundamentals", McGraw-Hill, Inc, 1988.

[4]. Lee S. and Bae C., "Design of a Heat Exchanger to Reduce the Exhaust Temperature in a Spark-Ignition Engine", International Journal of Thermal Sciences, Vol. 47, 2008, pp.468-478.

[5]. Turner, J.W.G., Pearson, R.J., Curtis, R. and Holland B., "Improving Fuel Economy in a Turbocharged DISI Engine Already Employing Integrated Exhaust Manifold Technology and Variable Valve Timing", SAE 2008-01-2449, 2008.

[6]. Akima, K., Seko, K., Taga, W., Torii, K. and Nakamura, S., "Development of New Low Fuel Consumption 1.8L I-VTEC Gasoline Engine with Delayed Intake Valve Closing", SAE 2006-01-0192, 2006.

[7]. Kuhlbach, K., Mehring, J., Borrman, D. and Friedfeldt, R., "Cylinder Head with Integrated Exhaust Manifold for Downsizing Concepts", MTZ Vol. 70, 2009.

[8]. Eftekhar, M. and Keshavarz, A., "Reducing Emissions and Fuel Consumption of a Spark Ignition Engine by Utilizing Heat Exchangers in the Exhaust Gas Stream", J. Automobile Engineering, Proc. IMechE Vol. 225(6) Part D, jun, 2011, pp.760-770.

[9]. Taylor, J., Fraser, N. and Wieske, P., "Water Cooled Exhaust Manifold and Full Load EGR Technology applied to a Downsized Direct Injection Spark Ignition Engine", SAE 2010-01-0356, 2010.

[10]. Ngy Srun, A.P., "Exhaust Heat Exchange Coefficient in a Pipe of an Internal Combustion Engine: EGR Cooler and Passenger Compartment Heating Applications", SAE 2000-01-0966, 2000.

[11]. Lee, S.H., Bae, C.S., Jeon, J.I., and Han, T.S., "Effect of Design Parameters on the Performance of Finned Exhaust Heat Exchanger", SAE 2003-01-3076, 2003.

[12]. Choi. S.U.S, "Enhancing thermal conductivity of fluid with nanoparticles. In: Siginer, D.A., Wang, H.P. (Eds.), Developments and Applications of Non-Newtonian Flows", FED-V.231/ MD-V.66. ASME, New York, 1995, pp. 99–105.

[13]. Xiang-Qi Wang, Arun S.Mujumdar, "Heat transfer characteristic of nanofluids: a review", International Journal of Thermal Science 46, 2007, pp. 1-19.

[14]. Xuan, Y., and Li, Q., "Heat transfer enhancement of nanofluids", International Journal of Heat and Fluid Flow, 21 (1), 2000, pp. 58-64.

[15]. Xuan, Y. and Roetzel, W., "Conception for heat transfer correlation of nanofluid" International Journal of Heat and Mass Transfer, 43 (19), 2000, pp. 3701-3707.

[16]. S.B., Maiga, S.J., Palm, C.T., Nguyan, G., Roy, N., Galanis, "Heat transfer enhancement by using nanofluids in forced convection flows". Int. J. Heat Fluid Flow 26, 2005, pp.530–546.

[17]. S. Vajjha Ravikanth, K. Das Debendra, K. Namburu Praveen, "Numerical study of fluid dynamic and heat transfer performance of Al2O3 and CuO nanofluids in the flat tubes of a radiator", Int. J. Heat and Fluid Flow, 2010, pp. 613-621.

[18]. Ghasemian, A., Keshavarz, A. and Shokouhi, A., "Enhancement of Internal Combustion Engine Heat Transfer by using Nanofluid as a Coolant", 13th Annual & 2nd International Fluid dynamics, Shiraz University, Iran, FD2010 Oct.

[19]. Ghasemian, A. & Jazaiery, A., "Reduction of Warm-up Timing in SI Engine by Preheating the Components", JER Journal, 2010.

[20]. Veshagh, A. and Chen, C. "A Computer Model for Thermofluid Analysis of Engine Warm-Up Process" SAE paper 931157.

[21]. Bejan, A., "Entropy Generation Minimization", CRC Press, 1998.

[22]. Webb, R.L. and Scott, M.J., "A Parametric Analysis of the Performance of Internally Finned Tubes for Heat Exchanger Application", J. Heat Transfer, Vol. 102, 1980, pp. 38-43.

[23]. Carnavos, T.C., "Heat Transfer Performance of Internally Finned Tubes in Turbulent Flow", Heat Trans. Eng., 4(1), 1980, pp. 32-37.

[24]. Jensen, M.K. and Vlakancic, A., "Experimental Investigation of Turbulent Heat Transfer and Fluid Flow in Internally Finned Tubes", Int. J. Heat Mass Transfer, Vol. 42, 1999, pp. 1343-1351.

[25]. Srinivasan, V. and Christensen, R.N., "Experimental Investigation of Heat Transfer and Pressure Drop Characteristics of Flow Through Spirally Fluted Tubes", Exp. Thermal Fluid Sci., Vol. 5, 1992, pp. 820-827.

[26]. Arnold, J.A., Garimella, S., and Christensen, R.N., "Fluted Tube Heat Exchanger Design Manual", GRI Report 5092–243–2357, 1993.

[27]. [27] Liu, X. and Jensen, M.K., "Geometry Effects on Turbulent Flow and Heat Transfer in Internally Finned Tubes", J. Heat Transfer, Vol. 123, 2001, pp. 1035-1044.

[28]. [28] Eftekhar, M., "Design of Optimum Heat Exchanger to Reduce the Exhaust Gas Temperature at High loads and the Warm up Timing", M.S. thesis, K.N. Toosi University of Technology, 2010.

[29]. Hamilton, R.L. and Crosser, O.K. "Thermal conductivity of heterogeneous two component system, I and EC Fundamentals 1", 1962, pp. 187-191.

[30]. Nguyen, C.T., "Temperature and particle-size dependent viscosity data for water-based nanofluids-hysteresis phenomena", International Journal of Heat and Fluid Flow 28, 2007, pp.1492-1506.

[31]. Pak, B.C. and Cho, Y.I., "Hydrodynamic and heat transfer study of dispersed fluids with submicron metallic oxide particles, Exp". Heat Transfer 11, 1998, pp.151-170.

[32]. Buongiorno, J. "Convective transport in nanofluids", Journal of Heat Transfer, 128, 2006, pp. 240-250.

[33]. ASHRAE, "Handbook Fundamentals", American Society of Heating, Refrigerating and Air-Conditioning Engineers Inc., Atlanta, 2005.

[34]. Touloukian, Y.S. "Thermophysical Properties of High Temperature Solid Al2O3 Materials", vol.4. Pt 1, sec.1, pp.8-47.

[35]. Shames, I. H., "Mechanics of fluids", 4th Edition, McGraw Hill, 2003.

[36]. Shayler, P. J. and Christian, S. J. "A Model for the Investigation of Temperature, Heat Flow and Friction Characteristics during Engine Warm-Up" SAE paper 931153.